*Indian J Phys (April 2017) 91(4):431–438*
DOI 10.1007/s12648-016-0940-8

ORIGINAL PAPER

# Characteristics study of projectile's lightest fragment for $^{84}Kr_{36}$–emulsion interaction at around 1 A GeV

**N Marimuthu[1,2], V Singh[1]* and S S R Inbanathan[2]**

[1]Physics Department, Institute of Science, Banaras Hindu University, Varanasi 221005, India

[2]Post Graduate and Research Department of Physics, The American College, Madurai, Tamilnadu 625002, India

Received: 29 March 2016 / Accepted: 24 August 2016 / Published online: 20 December 2016

**Abstract:** In this article, we present the results of our investigations on the projectile's lightest fragment (proton) multiplicity and probability distributions with $^{84}Kr_{36}$ emulsion collision at around 1 A GeV. The multiplicity and normalized multiplicity of projectile's lightest fragment (proton) are correlated with the compound particles, shower particles, black particles, grey particles; alpha (helium nucleus) fragments and heavily ionizing charged particles. It is found that projectile's lightest fragment (proton) is strongly correlated with compound particles and shower particles rather than other particles and the average multiplicity of projectile's lightest fragment (proton) increases with increasing compound, shower and heavily ionizing charge particles. Normalized projectile's lightest fragment (proton) is strongly correlated with compound particles, shower particles and heavily ionizing charge particles. The multiplicity distribution of the projectile's lightest fragment (proton) emitted in the $^{84}Kr_{36}$ + emulsion interaction at around 1 A GeV with different target has been well explained by KNO scaling. The mean multiplicity of projectile's lightest fragments (proton) depends on the mass number of the projectile and does not significantly dependent of the projectile energy. The mean multiplicity of projectile's lightest fragment (proton) increases with increasing the target mass number.

**Keywords:** Nuclear emulsion; Projectile's lightest fragment (proton); KNO scaling; Multiplicity and normalized multiplicity

**PACS Nos.:** 25.75.-q; 29.40.Rg; 25.70.Mn; 25.70.Pq

## 1. Introduction

In recent times experimental high energy physicists are trying to understand the multifragmentation process and the interactions with target—nucleus to provide some aspects of nuclear structure [1, 2]. Nuclear emulsion detector (NED) technique is one of the important tools for intermediate and high energy physics. This is understood through a long list of fundamental discoveries. For the last several years, nuclear emulsion techniques are in use to investigate nucleus–nucleus and nucleus–hadrons collisions, and neutrino interactions. This is due to the fact that the nuclear emulsion detector provides $4\pi$ geometry and sub-micron spatial resolution, and also its excellent detection efficiency of relativistic particles. In the past few decades, large number of researchers has investigated the multiplicity distribution and multiplicity correlation with evaporated and recoil nucleons of target, produced mesons, helium and heavily ionizing charged particles [3–9]. It is believed that, it may help us to understand the interaction mechanism and rare particle production. The fragmentation has been one of the most important aspects of nucleus–nucleus collision and hadrons–nucleus collision. According to the participant–spectator model [10–13], heavy ion interaction regions are called as "participant region" and rest are spectators. During collision, in the participant region, we may expect the local density and temperature to increase and after that the participant region expands and eventually cools down. The single charged relativistic particles and rare isotopes are formed from participant region. These are mostly mixture of pions, k-mesons and less proportional to the fast protons. The target fragment is formed from the target-spectator. The target fragment is the combination of recoiled proton and evaporated fragments

*Corresponding author, E-mail: venkaz@yahoo.com

from target-spectator region. According to the emulsion detector terminology, the target recoiled nucleons are called as grey particles and evaporated target fragments are black particles. The projectile fragments formed from the highly excited projectile-spectator residues through the evaporation. The projectile fragments belong to the projectile-spectator region of the collision geometry and the projectile's lightest fragment (proton) is expected to come from the highly excited portions of the projectile-spectator. It may carry the information about the equation of state, dynamical mechanism and liquid phase transition of low density matter [2, 14]. So it is very important to investigate projectile's lightest fragment (proton). In this paper, we have focused on the complete investigation of the projectile's lightest fragment (proton) multiplicity and its correlation with other secondary particles of $^{84}Kr_{36}$ with NIKFI-BR2 emulsion plates at kinetic energy around 1 GeV per nucleon.

## 2. Experimental details

For the present experiment, high sensitive stack of NIKFI-BR2 emulsions plates, having unprocessed thickness of 600 μm, plates were exposed horizontally with the beam of $^{84}Kr_{36}$ having kinetic energy around 1 GeV per nucleon at the edge of the plate. This was performed at Gesellschaft fur Schwerionenforschung (GSI) Darmstadt, Germany. The events/interactions were observed through the line scanning technique with oil immersion objective lens of 100× along with the 15× eyepieces. There are two types of scanning methods used to study the emulsion plates; one is line scanning and the other one volume scanning. In the line scanning method the beam tracks are picked up at 5 mm distance from the edge of emulsion plate and it is carefully followed, since they are interacting with the nuclear emulsion nuclei or escaped from any sides of the emulsion plate. To make sure that we are following primary track, first, we followed the track in the backward direction till the edge of the plate. In the volume scanning methods, the information is collected through strip by strip scanning [6–8]. The first interaction/event observed are the primary interaction and emitted particles are the secondary one. According to the emulsion terminology, the emitted secondary charged particles are classified through their range, velocity and ionization, and classified in the following categories.

### 2.1. Black particles

The black particles are evaporated target fragments. Most of them are produced from the residue of target nuclei and their range <3 mm. The relativistic velocity of the particles is 0.3 c and their kinetic energy <20 MeV. The multiplicity of black particles is denoted as $N_b$.

### 2.2. Grey particles

These particles are mostly recoil proton of target and their range should be greater than 3 mm. These particle have relativistic velocity $0.3c < \beta < 0.7c$ and their kinetic energy $30 < E < 400$ MeV. The multiplicity of these particles is denoted as $N_g$.

### 2.3. Shower particles

These particles are singly-charged freshly created relativistic particle. These particles come from the participant region and their velocity is greater than 0.7c. These are mainly pions and kaons, and contaminated with less number of fast protons. The multiplicity of shower particles is denoted as $N_s$.

A set of these particles form a new parameter called compound particles defined as a sum of recoil proton and shower particles and their multiplicity denoted as $N_c = (N_g + N_s)$.

### 2.4. Heavily ionizing charged particles

These charged particles are the part of target nucleus or group of the target fragments. The multiplicity of heavily ionizing charged particles denoted as $N_h$ and is equal to the sum of black and gray particles $N_h = (N_b + N_g)$.

### 2.5. Projectile fragments

The projectile fragments are spectator part of the projectile nucleus or projectile spectators. All the projectile fragments are emitted in the narrow forward cone of $\pm 8^{\circ}$. In the present work, the projectile fragments have been categorized on the basis of their charge as follows:

1. Singly charged projectile fragments or projectile's lightest fragment (proton)—These are mostly projectile proton ($PF_{Z=1}$) and velocity of this particle is almost equal to the beam velocity. It is denoted as $N_p$.
2. Alpha projectile fragments—These particles are doubly charged projectile fragments ($PF_{Z=2}$) and are basically Helium nuclei. It is presented as $N_{Alpha}$.
3. Heavy projectile fragments—These particles are multiple charged projectile fragments ($PF_{Z>2}$) and is presented as $N_f$.

## 3. Results and discussion

In the present paper, we have investigated 892 primary inelastic events chosen from the $^{84}Kr_{36}$–emulsion interaction at around 1 A GeV. Initially we have carried out the target identification for $^{84}Kr_{36}$–emulsion interactions, since

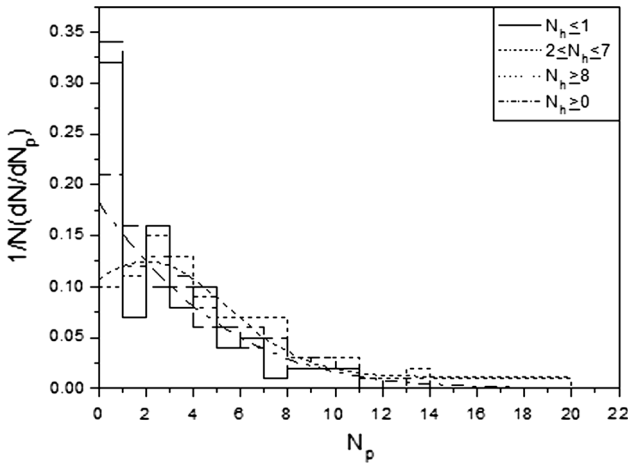


**Fig. 1** The multiplicity distribution of projectile's lightest fragment (proton) ($N_p$) for the different target groups in the $^{84}Kr_{36}$–emulsion interactions at around 1 A GeV are plotted

**Table 1** Gaussian distribution parameter values for different targets

| Interactions | Peaks value | Width |
|---|---|---|
| H ($N_h \leq 1$) | −0.417 | 1.182 |
| CNO ($2 \leq N_h \leq 7$) | −7.974 | 7.164 |
| Ag/Br ($N_h \geq 8$) | 2.013 | 6.816 |
| Kr–emulsion ($N_h \leq 0$) | −13.153 | 17.265 |

the exact target identification is not possible in case of NED because the nuclear emulsion medium is composed of the H, CNO and Ag/Br compounds and molecules. However, we have classified target groups statistically on the basis of heavily ionizing charged particle ($N_h$) multiplicity for each event. The $N_h \leq 1$ events taken to be $^{84}Kr_{36}$–H interaction, events with $2 \leq N_h \leq 7$ are $^{84}Kr_{36}$–CNO interactions and events having $N_h \geq 8$ are $^{84}Kr_{36}$–Ag/Br interactions. The number of events corresponding to these interactions is 136, 300 and 456, respectively. Multiplicity distribution of projectile's lightest fragment (proton) produced in $^{84}Kr_{36}$–emulsion at around 1 A GeV interactions is shown in Fig. 1.

Here the target Ag/Br and $^{84}Kr_{36}$–emulsion interactions distributions are fitted with the Gaussian function. The maximum $N_p$ values are extended up to 11, 11, 20 and 20 for H, CNO, Ag/Br and emulsion targets, respectively. The distributions of projectile's lightest fragment (proton) shapes are almost similar for different targets, whereas the distribution becomes wider with increase of target mass. The Gaussian distribution parameter values for different targets are tabulated in Table 1.

Table 2 shows the mean multiplicity of the projectile's lightest fragments (proton) for different target groups of $^{84}Kr_{36}$–emulsion interactions at around 1 A GeV. In order to compare the similar parameter results of other projectiles are also listed. One can easily see, from this table, that the mean multiplicity of projectile's lightest fragment (proton) for different target groups increases with increase in the average target mass number and also its decrease by increasing the projectile kinetic energy.

Figure 2 depicts the probability distribution of projectile light fragment (proton) fitted with the Gaussian distribution function. The maximum value of probability is found to be 21.74 ± 2.2 with the peaks and the width of the Gaussian function is −10.07 and 16.28, respectively. The probability distribution of projectile lightest fragment (proton) extends up to 20 in an event. Various separate regions can be seen in the probability distribution of $N_p$ as shown in Fig. 2. It seems that these regions are belonging to the target groups of nuclear emulsion detector. Regions are marked in Fig. 2 roughly according to the target groups.

Data presented in the Table 3 shows the average multiplicities of projectile's lightest fragment (proton) ($<N_p>$) for different projectiles of similar and different kinetic energy. From this table, it is observed that the mean multiplicity of the projectile's lightest fragment (proton) completely depends on mass number of the projectile ($A_p$), but not on kinetic energy of the projectile ($E_p$). The mean multiplicity of projectile's lightest fragment (proton) decreases with increasing projectile kinetic energy. We have also studied the dependence of average multiplicity of

**Table 2** Mean multiplicity of the projectile lightest fragment (proton) for different target groups and projectiles of similar and different kinetic energy

| Projectile | Energy (A GeV) | $<N_p>$ | | | |
|---|---|---|---|---|---|
| | | H | CNO | AgBr | References |
| $^{12}C$ | 3.7 | 0.77 ± 0.07 | 1.12 ± 0.04 | 0.86 ± 0.02 | [23] |
| $^{22}Ne$ | 3.3 | 1.17 ± 0.02 | 1.47 ± 0.04 | 1.37 ± 0.03 | [21] |
| $^{56}Fe$ | 1.0 | 2.53 ± 0.29 | 3.19 ± 0.28 | 4.94 ± 0.44 | [15] |
| $^{56}Fe$ | 1.7 | 2.35 ± 0.17 | 3.00 ± 0.13 | 3.03 ± 0.09 | [22] |
| $^{84}Kr$ | 1.7 | 2.44 ± 0.21 | 2.67 ± 0.15 | 3.06 ± 0.16 | [18] |
| $^{84}Kr$ | 1.0 | 2.29 ± 0.59 | 3.55 ± 0.32 | 5.92 ± 0.62 | Present work |
| $^{132}Xe$ | 1.0 | 1.9 ± 0.3 | 4.7 ± 0.3 | 6.7 ± 0.3 | [20] |

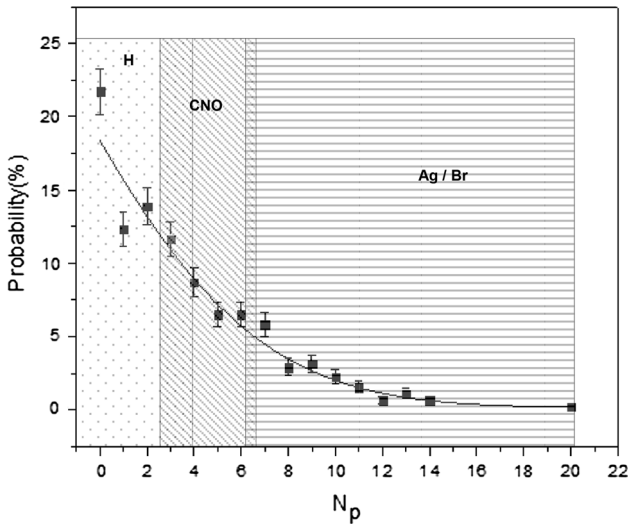


**Fig. 2** The probability distribution of the projectile's lightest fragment (proton) ($N_p$) for $^{84}Kr_{36}$–emulsion interactions at around 1 A GeV is shown. Various target regions are marked in the plot to guide the eyes

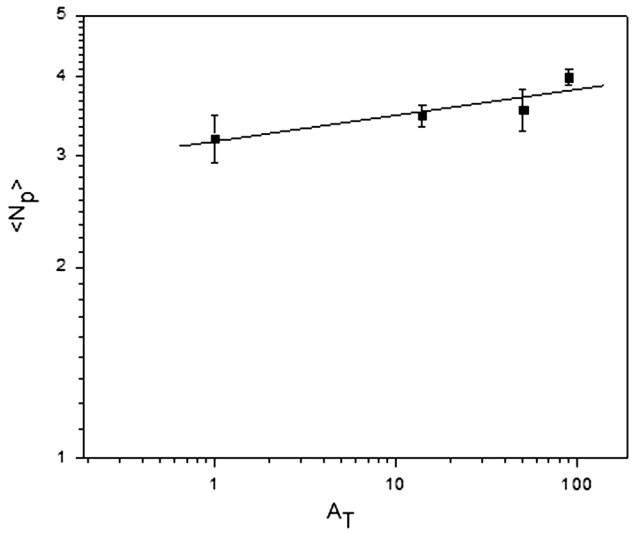


**Fig. 3** The average multiplicity of projectile's lightest fragment (proton) <$N_p$> is plotted as a function of target mass number ($A_T$)

**Table 3** The average multiplicities of projectile's lightest fragment (proton) for different projectile–emulsion inelastic interactions are listed

| Projectile | Energy (*A* GeV) | <$N_p$> | References |
|---|---|---|---|
| $^{4}$He | 3.7 | 0.61 ± 0.02 | [16] |
| $^{12}$C | 3.7 | 1.20 ± 0.04 | [16] |
| $^{12}$C | 3.7 | 0.62 ± 0.03 | [19] |
| $^{12}$C | 3.7 | 0.93 ± 0.02 | [23] |
| $^{16}$O | 3.7 | 1.45 ± 0.03 | [16] |
| $^{16}$O | 3.7 | 1.15 ± 0.08 | [17] |
| $^{22}$Ne | 3.3 | 1.55 ± 0.02 | [16] |
| $^{22}$Ne | 3.3 | 1.36 ± 0.02 | [21] |
| $^{28}$Si | 3.7 | 2.54 ± 0.05 | [16] |
| $^{28}$Si | 3.7 | 1.82 ± 0.05 | [19] |
| $^{84}$Kr | 1.7 | 2.79 ± 0.10 | [18] |
| $^{84}$Kr | 1.0 | 3.55 ± 0.16 | Present work |
| $^{132}$Xe | 1.0 | 4.6 ± 0.2 | [20] |

projectile's lightest fragment (proton) (<$N_p$>) with the average mass number of the target groups ($A_T$) as shown in the Fig. 3. It may be seen from Fig. 3 that the average multiplicity of projectile's lightest fragment (proton) (<$N_p$>) increases with increase of target mass number ($A_T$). These values are fitted with the linear best fit relation and the value of the fit parameter are given below.

$$<N_p> = (3.1514 \pm 0.1758)\, A_T^{(0.3337 \pm 0.1239)} \quad (1)$$

It can be seen from Eq. (1) that the average multiplicity of projectile's lightest fragment (proton) (<$N_p$>) has nearly cube root dependence of $A_T$.

### 3.1. KNO scaling for projectile's lightest fragment (proton) <$N_p$>

One of the dominant frame works to study the behavior of multiplicity distribution of secondary particles in nucleus–nucleus and hadrons–nucleus collisions is Koba–Nielson–Olesen (KNO) [24–27]. This is scaling consequence of nuclear geometry and explains the multiplicity distribution of secondary particles both experimentally and theoretically. The KNO scaling hypothesis is derived from the Feynman scaling of inclusive particle production cross section. According to the KNO scaling

$$\psi(Z) = 4Z\, exp\,(-2Z) \quad (2)$$

where

$$\psi(Z) = <N_p> P(N_p) = <N_p> \sigma_{np}/\sigma_{inels} \quad (3)$$

Here ψ (Z) is the energy independent function Z = $N_p$/<$N_p$>. Where $N_p$ refers to the event by event production of singly charged projectile fragments (proton) and <$N_p$> represents the average or mean multiplicity of projectile's lightest fragment (proton) for the whole data sample. $\sigma_{np}$ is referred to as the partial cross section of the produced charged particle of projectile's lightest fragment (proton) multiplicity ($N_p$) for the specific channel and $\sigma_{inels}$ is the total cross section. We know that ψ is energy independent, so it is approximately constant for all beam of same energy. In Fig. 4, we have plotted the multiplicity distribution <$N_p$>$\sigma_{np}/\sigma_{inels}$ versus the $N_p$/<$N_p$> for different target groups such as $^{84}Kr_{36}$–H, $^{84}Kr_{36}$–CNO, $^{84}Kr_{36}$–Ag/Br and $^{84}Kr_{36}$–emulsion interactions at around 1 A GeV. The experimental data point $N_p = 0$ has been excluded here. The experimental data is fitted with the universal function

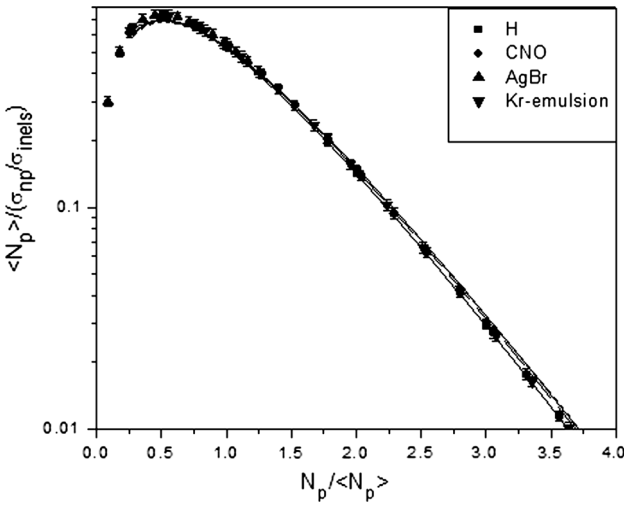


**Fig. 4** The KNO scaling distribution for the projectile's lightest fragment (proton) for the $^{84}Kr_{36}$–emulsion interactions at around 1 GeV per nucleon is plotted. The solid line represent the theoretical (KNO) fitting on the experimental data points ($N_p = 0$ excluded) with the function as shown in Eq. (4)

$$\psi(Z) = AZ\,exp^{(-BZ)} \tag{4}$$

From Fig. 4, one can see that most of the experimental data are laid on the universal curve and complete range of the spectrum is fitted well within the experimental error. The values of best fitting parameters A and B are obtained and are tabulated in Table 4. From Table 4, the fitting values of A and B are agreeing well with the theoretical one within the statistical error i.e. A = 4 and b = 2. The KNO fitting parameters of $^{84}Kr_{36}$–emulsion interactions at around 1 A GeV for different target values are compared with the $^{84}Kr_{36}$–emulsion interactions at 1.7 A GeV as listed in the Table 4 too. Information obtained from Table 4 and Fig. 4 reflects that the projectile's lightest fragment (proton) for the $^{84}Kr_{36}$–emulsion interactions at around 1 GeV per nucleon is strictly obeying the KNO scaling law i.e. distribution is independent of incident kinetic energy for low energies.

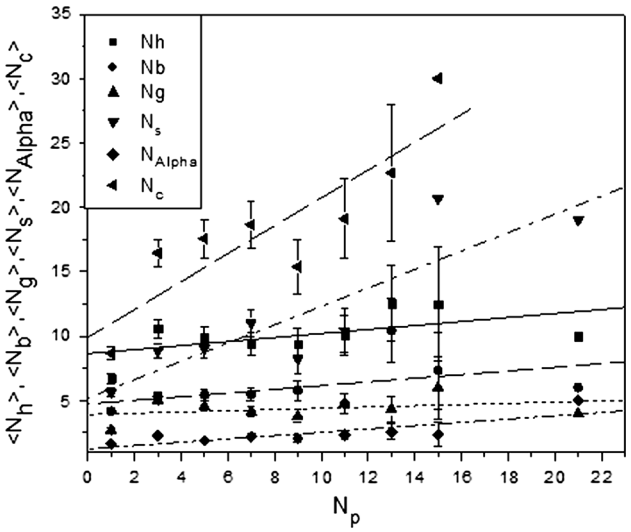


**Fig. 5** Multiplicity correlation between $<N_h>$, $<N_b>$, $<N_g>$, $<N_s>$, $<N_{Alpha}>$, and $<N_c>$ with $N_p$ for $^{84}Kr_{36}$–emulsion interaction at around 1 A GeV are plotted

### 3.2. Multiplicity correlation of $<N_h>$, $<N_b>$, $<N_g>$, $<N_s>$, $<N_{Alpha}>$, $<N_c>$ with $N_p$

The projectile's lightest fragments (proton) are coming from highly excited projectile residue and it might carry information about the collision dynamics. There are only few reports on the projectile's lightest fragments (proton) [15–23, 28]. Fig. 5 depicts the multiplicity correlation between secondary particles $<N_j> = <N_h>$, $<N_b>$, $<N_g>$, $<N_s>$, $<N_{Alpha}>$, $<N_c>$ and the number of projectile's lightest fragment (proton) ($N_p$) for $^{84}Kr_{36}$–emulsion interaction at around 1 A GeV. The symbols are experimental data with statistical error-bar and it is fitted with straight line function as mentioned in Eq. (5) and the fitting parameter values are tabulated in the Table 5.

Figure 5 reveals that, the average compound multiplicity ($<N_c>$) and shower particle multiplicity have strong correlation with the number of projectile's lightest fragment (proton) emitted in an event whereas the average

**Table 4** The values of the best fitting parameters of KNO scaling for $^{84}Kr_{36}$–emulsion interactions along with the different target groups at around 1 and 1.7 A GeV are tabulated

| Type of event | Energy (A GeV) | A | B | $\chi^2$/DoF | References |
|---|---|---|---|---|---|
| $^{84}$Kr–H | 1.7 | 3.28 ± 0.96 | 2.10 ± 0.24 | 0.783 | [18] |
| $^{84}$Kr–CNO | 1.7 | 3.00 ± 0.51 | 1.95 ± 0.13 | 0.392 | [18] |
| $^{84}$Kr–Ag/Br | 1.7 | 3.46 ± 0.66 | 2.08 ± 0.16 | 1.140 | [18] |
| $^{84}$Kr–Em | 1.7 | 3.36 ± 0.35 | 2.02 ± 0.08 | 0.501 | [18] |
| $^{84}$Kr–H | 1.0 | 3.61 ± 0.60 | 1.93 ± 0.28 | 0.309 | Present work |
| $^{84}$Kr–CNO | 1.0 | 3.7 ± 0.6 | 1.94 ± 0.28 | 0.321 | Present work |
| $^{84}$Kr–Ag/Br | 1.0 | 3.6 ± 0.6 | 1.95 ± 0.28 | 0.318 | Present work |
| $^{84}$Kr–Em | 1.0 | 3.6 ± 0.6 | 1.93 ± 0.28 | 0.309 | Present work |

**Table 5** The best fitting parameter's values are listed for the $^{84}Kr_{36}$–emulsion interactions at around 1 A GeV

| Type of event | a | B |
|---|---|---|
| $<N_h>$ | 8.64 ± 0.97 | 0.15 ± 0.08 |
| $<N_b>$ | 4.72 ± 1.08 | 0.14 ± 0.09 |
| $<N_g>$ | 3.91 ± 0.57 | 0.04 ± 0.05 |
| $<N_s>$ | 5.19 ± 1.72 | 0.71 ± 0.15 |
| $<N_{Alpha}>$ | 1.23 ± 0.38 | 0.12 ± 0.03 |
| $<N_c>$ | 9.9 ± 2.33 | 1.08 ± 0.25 |

multiplicities of black particles, grey particles, alpha particles, and heavily ionizing charged particles have shown weaker correlation with the number of projectile's lightest fragments (proton) i.e. $N_p$ emitted in an event. Table 5 suggests that the average multiplicity of compound particle and shower particles are rapidly increasing with the increase in the number of projectile's lightest fragment (proton). It is evident that the average multiplicity of recoil protons ($N_g$) and evaporated ($N_b$) target fragments are weakly dependent on the number of the projectile's lightest fragment (proton) which are coming from the participant region. The emission rate of the shower particles has a strong dependence on the number of projectile's lightest fragment (proton) showing almost similar source of origin i.e. participant region but according to the participant–spectator model emission of projectile fragments are strictly from the projectile spectator region. It means most of the singly charged projectile fragments are coming from the interface of participant and projectile spectator regions. The maximum number of compound multiplicity and shower particles emitted in an event is 15 and 21, respectively. The other particles like black, grey, alpha and heavily ionizing charged particles have not shown significant dependence on the projectile's lightest fragment (proton).

$$<N_j> \; = b<N_p> \; + a \tag{5}$$

### 3.3. Multiplicity correlation of $<N_p>$ with $N_c$, $N_s$, $N_{Alpha}$, $N_b$, $N_g$, and $N_h$

The multiplicity correlation of $<N_p>$ with the corresponding $N_c$, $N_s$, $N_{Alpha}$, $N_b$, $N_g$, and $N_h$ for $^{84}Kr_{36}$–emulsion interactions at around 1 GeV per nucleon are shown in Figs. 6 and 7 respectively. Here all the distributions are fitted with straight line function and the fitting parameters values are given in equation from Eqs. (6) to (9). From the Fig. 6, the average number of projectile's lightest fragment (proton) i.e. $<N_p>$ linearly increases with increasing number of shower particles ($N_s$). It means that majority of projectile's nucleons, especially protons in the present case, are emitted from the interface region of spectator and

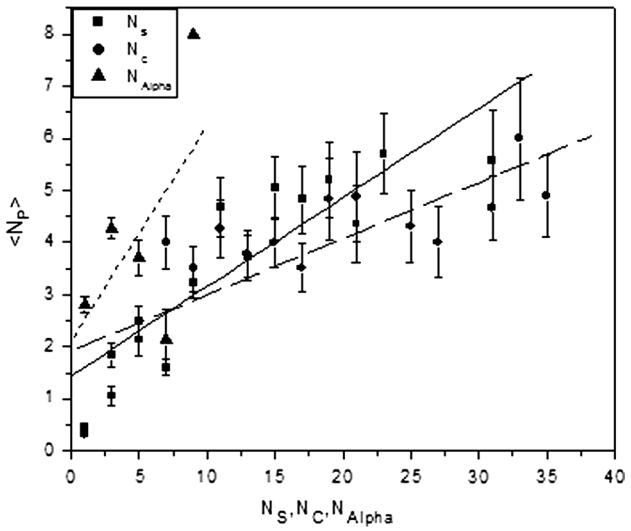


**Fig. 6** Multiplicity correlation between $<N_p>$ with $N_s$, $N_c$, and $N_{Alpha}$ for $^{84}Kr_{36}$–emulsion interactions at around 1 A GeV is plotted

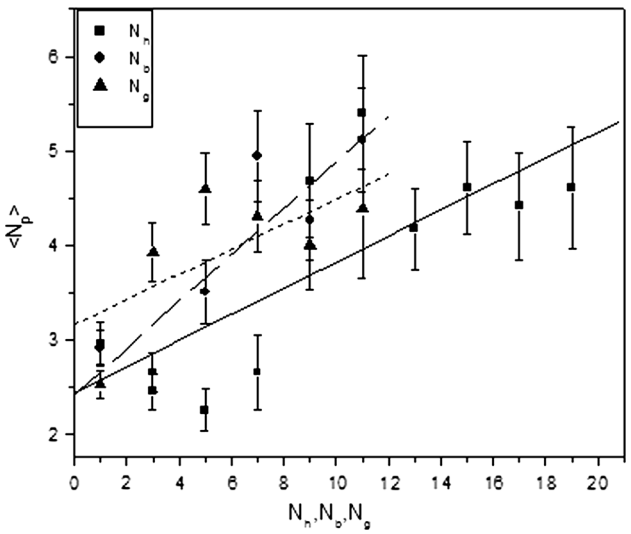


**Fig. 7** Multiplicity correlation between $<N_p>$ with $N_h$, $N_b$, and $N_g$ for $^{84}Kr_{36}$–emulsion interactions at around 1 A GeV is plotted

participant, and rest of the projectile's fragments is not even slightly involved in the violent process of the participant region. The $<N_p>$ value rapidly increases with increase in the number of compound particles ($N_c$) up to 21 $N_c$ per event and after that $N_c$ values have larger error bar due to less number of events in that $N_c$ region. The $<N_p>$ value initially increases with increasing the number of alpha particles in an event ($N_{Alpha}$).

From Fig. 7, we may see that the $<N_p>$ value rapidly increases with increasing number of black particles ($N_b$), grey particles ($N_g$) and heavily ionizing charge particles ($N_h$) up to 11 particles per event. This indicates the overall increase in the overlap volume of the target and projectile because target and projectile associated particles numbers

are increasing with similar strength. It may also be seen that, the $<N_p>$ values are saturated for ($N_h$) values beyond the 13 number of heavily ionizing charged particle. This plot indicates that heavily ionizing particles and grey particles show similar strength of the correlation with projectile's lightest fragment (proton). The slopes value for $N_h$ and $N_g$ are found to be ($0.13 \pm 0.04$) and ($0.13 \pm 0.01$), respectively.

The maximum number of $N_p$ observed in an event is 36, which is equal to the total charge of the projectile ($^{84}Kr_{36}$). The maximum number of $N_c$ and $N_s$ observed in an event are 31 and 35, respectively. In the case of $N_b$, $N_g$ and $N_h$ the $<N_p>$ values start from $2.95 \pm 0.24$, $2.91 \pm 0.10$ and $2.52 \pm 0.14$, respectively.

$$<N_p> = (0.17 \pm 0.02)N_s + (1.44 \pm 0.44) \quad (6)$$

$$<N_p> = (0.10 \pm 0.02)N_c + (1.93 \pm 0.43) \quad (7)$$

$$<N_p> = (0.41 \pm 0.34)N_{Alpha} + (2.12 \pm 1.96) \quad (8)$$

$$<N_p> = (0.13 \pm 0.04)N_h + (2.43 \pm 0.50) \quad (9)$$

$$<N_p> = (0.24 \pm 0.06)N_b + (2.41 \pm 0.43) \quad (10)$$

$$<N_p> = (0.13 \pm 0.01)N_g + (3.15 \pm 0.51) \quad (11)$$

### 3.4. Normalized multiplicity correlation of $<N_p>/N_p$ with $N_s$, $N_c$, $N_{Alpha}$, $N_h$, $N_b$, and $N_g$

Figures 8(a) and 8(b) depict the correlation between normalized multiplicity of projectile's lightest fragment (proton) i.e. $(1/N_p)*(d<N_p>/dN_i)$ with the $N_s$, $N_c$, $N_{Alpha}$, $N_h$, $N_b$, and $N_g$, here i = s, c, Alpha, h, b and g. These data are well fitted by linear function and the best fitting parameters values are listed in Table 6. From Fig. 8(a), the multiplicity of compound and shower particles has shown a strong correlation with normalized projectile's lightest fragment (proton). It can be seen that the normalized value of projectile's lightest fragment (proton) linearly increases with increasing number of shower particles ($N_s$). The normalized number of projectile's lightest fragment (proton) rapidly increases with the number of compound particle multiplicity ($N_c$) and after $N_c = 28$, it remarkably increases with the compound particles ($N_c$) multiplicity unlike the $<N_p>/N_p$ with the number of alpha ($N_{Alpha}$) particles emitted in an event.

From Fig. 8(b), the number of heavily ionizing charged particles ($N_h$), black particles ($N_b$) and the grey particles ($N_g$) have weak dependence with normalized multiplicity of projectile's lightest fragment (proton) from 1 to 9 but in this region normalized multiplicity of projectile's lightest fragment (proton) linearly increases with $N_h$, $N_b$, and $N_g$. It also shows that the number of $N_h$, $N_b$ and $N_g$ are equally interacting with H and CNO targets. Again the number of $N_h$ linearly increases with normalized multiplicity of

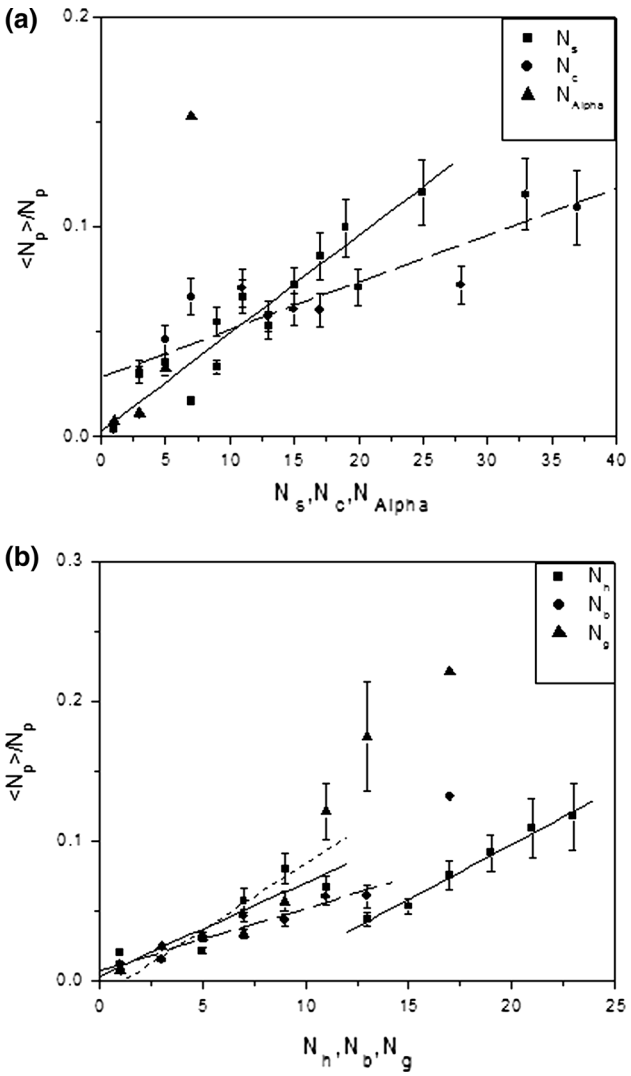


**Fig. 8** **(a)** Normalized multiplicity correlation between $<N_p>/N_p$ with the values of $N_s$, $N_c$, and $N_{Alpha}$ for $^{84}Kr_{36}$–emulsion interactions at around 1 A GeV are plotted **(b)** Normalized multiplicity correlation between $<N_p>/N_p$ with the values of $N_h$, $N_b$, and $N_g$ for $^{84}Kr_{36}$–emulsion interactions at around 1 A GeV are plotted

**Table 6** The best fitting values of parameters for normalized multiplicity correlation for $^{84}Kr_{36}$–emulsion interactions at around 1 A GeV are listed

| Type of event | a | b |
|---|---|---|
| $<N_s>$ | $0.0026 \pm 0.0063$ | $0.0046 \pm 4.76 \times 10^{-4}$ |
| $<N_c>$ | $0.0287 \pm 0.0068$ | $0.0022 \pm 3.622 \times 10^{-4}$ |
| $<N_{Alpha}>$ | $-0.0405 \pm 0.4425$ | $0.0228 \pm 0.0096$ |
| $<N_h>$ | $0.0040 \pm 0.0118$ | $0.0066 \pm 0.0017$ |
| | $-0.0595 \pm 0.0084$ | $0.0078 \pm 4.6229 \times 10^{-4}$ |
| $<N_b>$ | $0.0077 \pm 0.0041$ | $0.0044 \pm 5.1288 \times 10^{-4}$ |
| $<N_g>$ | $-0.0109 \pm 0.0170$ | $0.0095 \pm 0.0024$ |

projectile's lightest fragment (proton) beyond the value of 13 $N_h$ per event. It reflects that the heavily ionizing particles ($N_h$) not only equally interact with H and CNO target but are also strongly interacting with Ag/Br targets.

## 4. Conclusions

We have significantly investigated the projectile's lightest fragment (proton) multiplicity distribution, probability distribution and its normalized multiplicity correlated with the secondary particles. From this investigation, we may conclude that, the mean multiplicity of the projectile's lightest fragment (proton) ($<N_p>$) completely depends on the mass number of the projectile and does not show significant dependence on the projectile energy. The average multiplicity of the projectile's lightest fragment (proton) increases with increase in the target mass number ($A_T$). The multiplicity distribution of projectile's lightest fragment (proton) emitted in the $^{84}Kr_{36}$–emulsion interaction is well explained by the KNO scaling law and it is also obeying that law. The experimental data are well fitted with universal function and fitting values are almost close to the theoretical value within the statistical error. Correlation between $<N_h>$, $<N_b>$, $<N_g>$, $<N_s>$, $<N_{Alpha}>$, $<N_c>$ and projectile's lightest fragment (proton) $<N_p>$ have shown that, the average compound particles and shower particles show strong correlation with projectile's lightest fragment (proton) $<N_p>$ rather than the black particles, grey particles, alpha particles and heavily ionizing charged particles. The correlation between $N_c$, $N_s$, $N_{Alpha,}$ $N_b$, $N_g$, $N_h$ and $<N_p>$ shows that, the $<N_p>$ rapidly increases with increasing $N_c$, $N_s$ and $N_h$. In the case of $N_c$, the $<N_p>$ increases up to $N_C = 21$ after that $<N_p>$ starts decreasing with increasing $N_c$ values. The $<N_p>$ values are saturated for $N_h$ values beyond 13. The heavily ionizing charged particles and grey particles show similar strength on the projectile's lightest fragment (proton) within the statistical error bar. The slope values for $N_h$ and $N_g$ are $(0.13 \pm 0.04)$ and $(0.13 \pm 0.01)$, respectively. Normalized projectile's lightest fragment (proton) show a strong correlation with the compound particles, shower particles and heavily ionizing charged particles rather than the black particles, grey particles and alpha particles. Normalized projectile's lightest fragment (proton) linearly increases with increasing $N_h$, $N_g$ and $N_b$ values from 1 to 9. It shows that $N_h$, $N_g$ and $N_b$ are equally interacting with targets H and CNO.

**Acknowledgements** We are thankful to all the technical staff of GSI, Germany for exposing nuclear emulsion detector with $^{84}Kr_{36}$ beam. The authors are grateful to the DST, New Delhi for financial support.

## References

[1] M K Singh, A K Soma, R Pathak and V Singh *Indian J. Phys.* **88** 323 (2014)
[2] J-S Li, D-H Zhang, H-L Li and N Yasuda *Nucl. Instrum. Methods Phys. Res. B* **307** 503 (2013)
[3] B S Nilsen, C J Waddington, J R Cummings, T L Garrard, and J Klarmann *Phys. Rev. C* **52** 6 (1995)
[4] S A Krasnov *et al. Czechoslov. J. Phys.* **46** 6 (1996)
[5] M K Singh, A K Soma, R Pathak and V Singh *Indian J. Phys.* **87** 59 (2013)
[6] V Singh, S K Tuli, B Bhattacharjee, S Sengupta and A Mukhopadhyay arXiv:nucl-ex/0412049v1 (2004)
[7] N S Chouhan, M K Singh, V Singh and R Pathak *Indian J. Phys.* **87** 1263 (2013)
[8] M K Singh, R Pathak and V Singh *Indian J. Phys.* **84** 1257 (2010)
[9] A Abdelsalam and B M Badawy *J. Nucl. Radiat. Phys.* **3** 109 (2008)
[10] J Knoll and J Hufner *Nucl. Phys. A* **308** 500 (1978)
[11] M Gauylassy and S K Kauffmann *Phys. Rev. Lett.* **40** 298 (1978)
[12] R R Joseph, I D Ojha and S K Tuli *J. Phys. G Nucl. Part Phys.* **15** 1805 (1989)
[13] M K Singh, A K Soma, R Pathak and V Singh *Indian J. Phys.* **85** 1523 (2011)
[14] B Bhattacharjee, A Mukhopadhyay, V Singh, S K Tuli and S Sengupta *Radiat. Meas.* **36** 291 (2003)
[15] E Firu *et al. Roman. Rep. Phys*. **63** 425 (2011)
[16] S Fakhraddin and M A Rahim *Phys. Scr.* **78** 015101 (2008)
[17] F-H Liu *Chin. J. Phys.* **41** 486 (2003)
[18] B Cai-Yan and Z Dong-Hai *Chin. Phys. C* **35** 436 (2011)
[19] M Tariq, M Zafar, A Tufail and S Ahmad *Int. J. Mod. Phys. E* **4** 347 (1995)
[20] E S Basova, V S Navotny, N V Petrov, T P Trofimova and B P Tursunov *Phys. At. Nucl.* **60** 1650 (1997)
[21] N P Andreeva, Z V Anzon and V I Bubnov *Sov. J. Nucl. Phys.* **47** 102 (1988)
[22] G M Chernov, K G Gulamov, U G. Gulyamov, V S Navotny, N V Petrov and L N Svechnikova *Nucl. Phys. A* **412** 534 (1984)
[23] R A Bondarenko, K G Gulamov, U G Gulyamov and G M Chernov *Sov. J. Nucl. Phys.* **38** 903 (1983)
[24] Z Koba, H B Nielsen and P Olesen *Nucl. Phys. B* **40** 317 (1972)
[25] P L Jain and M M Aggarwal *Phys. Rev. C* **33** 5 (1986)
[26] F-H Liu and Y A Panebratsev *Il Nuov. Cimen. Note. Bre*. **111** 10 (1998)
[27] F-H Liu *Phys. Rev. C* **62** 024613 (2000)
[28] V Singh PhD Thesis (Banaras Hindu University Varanasi, India) (1998)